Engineering Journal issn: 0125-8281

Article

Data-Driven Solutions for Backcalculating Elastic Moduli of Flexible Pavements from FWD Test

Barami Phulsawat[1,a], **Teerapong Senjuntichai**[1,b,*], **Angsumalin Senjuntichai**[2,c], **and Wichirat Kaewjuea**[3,d]

1 Center of Excellence in Applied Mechanics and Structures, Department of Civil Engineering, Faculty of Engineering, Chulalongkorn University, Bangkok, 10330, Thailand
2 Department of Industrial Engineering, Faculty of Engineering, Chulalongkorn University, Bangkok, 10330, Thailand
3 Department of Civil Engineering, Faculty of Engineering, Prince of Songkla University, Songkhla 90110, Thailand
E-mail: [a]barami8580@gmail.com, [b,*]teerapong.s@chula.ac.th (Corresponding author), [c]angsumalin.s@chula.ac.th, [d]wichairat@gmail.com

Abstract. Traditional methods for calculating pavement layers elastic moduli from falling weight deflectometer (FWD) tests often rely on computationally intensive iterative processes and lack struggle to capture complex variable relationships. This article highlights the utilization of machine learning (ML) algorithms, which include artificial neural networks (ANN), long-short-term memory (LSTM), and random forests (RF), to predict the elastic moduli of multi-layered flexible pavement based on FWD test. All ML algorithms were developed using synthetic databases derived from the exact stiffness matrix scheme, which was employed for the analysis of multi-layered pavements under axisymmetric surface loading. The development of ML models involves preprocessing of data, hyperparameter optimization, and performance evaluation. The input variables consist of the FWD surface deflections, the magnitude of applied loading, and the layer thicknesses, while the output variables represent the predicted layered elastic moduli of the pavement structure. The ANN and LSTM models capture complicated relations more effectively than the RF model in the backcalculation of the layered elastic modulus based on the FWD test. Among the two, LSTM achieves higher accuracy, with the average values across all layer moduli of R^2 and MAPE being 99.04% and 2.41%, respectively, in the test set. The applicability of LSTM model is further demonstrated by comparing with the backcalculated elastic modulus based on the FWD field experiments performed on the infrastructure of roads in Thailand. Furthermore, a sensitivity analysis reveals that deflections near the center of loading predominantly impact the predictions of upper layer moduli, while the moduli of lower layers are influenced by deflections across all geophones.

Keywords: Artificial neural networks, backcalculation, data-driven solutions, flexible pavements, FWD, long-short term memory, sensitivity analysis.

ENGINEERING JOURNAL Volume 29 Issue 3
Received 16 August 2024
Accepted 5 March 2025
Published 31 March 2025
Online at https://engj.org/
DOI:10.4186/ej.2025.29.3.27

1. Introduction

Machine learning (ML), a fundamental component of artificial intelligence (AI), plays a pivotal role in terms of innovation in technology, profoundly influencing the problem-solving and decision-making strategies across various disciplines. Fundamentally, machine learning enables systems to enhance their performance and learn from experience or data autonomously, without the need for explicit programming instructions. The influence of machine learning extends beyond individual capabilities, influencing numerous industries like healthcare, finance, education, etc. The capacity of machine learning (ML) to process intricate and extensive datasets has brought about a paradigm shift in the field, enabling engineers to devise solutions for problems with greater accuracy and efficacy. In the past, machine learning approaches were implemented to address a wide range of civil engineering problems [1-6].

Significant consideration has been paid to the utilization of ML to enhance the capabilities of pavement engineering, a critical component of transportation infrastructure [7, 8]. The structural integrity of pavement systems is contingent upon precise evaluations of material properties and performance, as they are essential for the preservation of safe and efficient transportation networks [9]. Falling weight deflectometer (FWD) assessments of roadway structural properties is the once most widely used test with regard to the rehabilitation and maintenance of multi-layered pavement structures. The accurate appraisal of layer properties is essential for cost-effective rehabilitation of pavements, which are critical infrastructure components. FWD is a non-destructive test that measures surface deflections at several points induced by the applied surface loading from the FWD device to backcalcultate the elastic moduli of layered pavements. Backcalculation scheme traditionally involves an iterative process, which requires complex analytical procedures and optimization algorithms, to deduce the pavement layer properties from the surface deflection data. However, conventional backcalculation methods are computationally intensive and have a limited ability to capture the complex relationships between variables.

In the past thirty years, a number of researchers have adopted soft computing techniques to overcome these challenges for the specific requirements of pavement engineering as a viable and effective substitute methodology for backcalculating pavement performance from FWD data. For example, Mier and Rix [10, 11] developed artificial neural network (ANN) models to estimate the elastic modul of flexible pavements. Sharma and Das [12] and Gonzalez et al. [13] later proposed ANN models to backcalculate elastic moduli of multi-layered pavements using synthetic deflection data. An ANN-based backcalculation model was also devised by Leiva-Villacorta et al. [14] to predict pavement layer moduli under both bonded and interface conditions for a full-slip layer. Furthermore, Ghanizadeh and Padash [15] developed a hybrid artificial neural network and the colliding body optimization algorithms (ANN-CBO) method to predict the elastic moduli of pavements using FWD dataset obtained from MICHPAVE program. Ghanizadeh et al. [16] developed an ANN model for estimating the elastic moduli of pavement layers, utilizing surface deflection datapoint acquired from FWD devices through the implementation of a non-PAS program. Ghanizadeh et al. [17] sequentially established a hybrid ANN-Jaya optimization algorithm to conduct a backcalculation procedure for the flexible pavement moduli. Additionally, Han et al. [18] presented a hybrid neural network framework for the backcalculation process to estimate the elastic moduli from the Long-Term Pavement Performance (LTPP) database.

The above review suggests that the development of data-driven solutions for the backcalculation process from FWD test has primarily concentrated on ANN-based models. Additionally, the consideration of appropriate hyperparameter optimization for ANN model was not widely addressed. Recently, an ML model based on random forest (RF) algorithm was proposed by Phulsawat et al. [19] to predict the modulus of elasticity of pavement layers from FWD experiment of the four-layered pavement, utilizing synthetic data of surface deflections generated from the exact stiffness matrix method [20-23]. The comparison between RF and ANN models with optimal values of hyperparameters generated by Phulsawat et al. [19] reveals that RF model performs better in terms of accuracy and computational expense in the estimation of the elastic moduli of multi-layered pavement based on FWD test data. Since the surface deflections measured at various geophones are strongly related [19], and the observed deflections are influenced by multiple factors, including pavement geometry and applied loading, these inherent dependency factors are difficult to capture using traditional schemes. Among various ML algorithms, Long Short-Term Memory (LSTM) networks have emerged as a particularly effective model for analyzing highly dependent data.

The current study utilizes LSTM models to capture complex and nonlinear relationships for predicting the elastic moduli of flexible multi-layered pavement. Additionally, ML models based on ANN and RF are also developed for comparison. The development process considers variations in layer thickness, the magnitude of applied loading, and measured surface deflections to improve model performance for preventive pavement maintenance in real-world scenarios, ultimately enhancing predictive accuracy and reliability. The multi-layered flexible pavement under consideration is a four-layer pavement structure commonly found in Thailand's road infrastructure, consisting of three separate layers of asphaltic concrete, base, and subbase over a subgrade material, as depicted in Fig. 1. Unlike the previous study [19], the thicknesses of the pavement layers and the applied loading have also been varied, in addition to the layered elastic moduli, in the creation of the synthetic database. All ML models are developed utilizing a dataset of 20,000 synthetic datapoints obtained from a conceptual

framework of FWD based on the exact stiffness matrix method [19-23]. The assessment of model performance encompasses a variety of statistical metrics. The aforementioned metrics comprise the root mean square error (RMSE), mean absolute percentage error (MAPE), and coefficient of determination (R^2), a20_index, ratio of root mean square error to observations' standard deviation (RSR), and index of scatter (IOS). The applicability of the developed model is further demonstrated by comparing the output from the LSTM-based model with the backcalulated elastic modulus based on the FWD experiments carried out on Thailand's road infrastructure. Finally, the analysis of sensitivity is performed to present the relative significance of the deflections measured at each location from FWD test on the estimation of the elastic moduli of multi-layered flexible pavements.

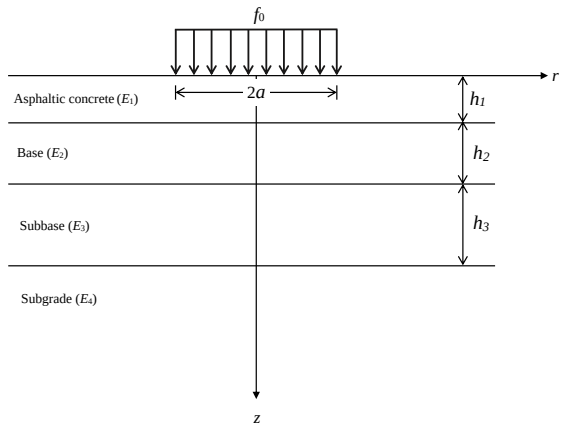

Fig. 1. Multi-layered pavement structure considered in the current study.

2. Soft-Computing Techniques

2.1. Artificial Neural Network (ANN)

The artificial neural network (ANN) was first proposed by McCulloch and Pitts [24] and subsequently developed by Metropolis et al. [25]. An ANN model is made up of three separate parts: each containing several neurons. These neurons are tasked with processing and transferring information through weighted connections, which incorporate the bias terms. The architectural framework of the ANN technique employed in this investigation is illustrated in Fig. 2. The thirteen neurons, identified as the applied loading (f_0), the layer thicknesses (h_1, h_2, h_3), and the nine surface deflections (D_1-D_9), constitute the input layer of this investigation. The hidden layer executes complicated computations and transformations on the data, capturing patterns and relationships. Each hidden layer consists of multiple layers, each of which contains numerous neurons. The predicted modulus of elasticity for multi-layered flexible pavement is provided by the output layer, which has four neurons. The subsequent expression represents the equation of the activation function of the feed-forward neural network:

$$a_i^l = f\left(\sum_{j=1}^{L} w_{ji}^l a_j^{l-1} + b_i^l\right) \quad (1)$$

where a_i^l represents the output value resulting from passing their connection weight through a transfer function as an input; L represents the quantity of connections to the preceding layer; w_{ji}^l denotes to the weights parameter of the connection between layer; b_i^l is constant of the bias term; and f is a transfer function (activation function).

Each neuron in a hidden layer computes a weighted sum of its inputs, incorporates a bias, and implements the result through a transfer function by using Eq. (1). As transfer functions, the rectified linear units (ReLU) and hyperbolic tan (tanh) functions are trialed in this article to obtain an optimal function with the highest predictive accuracy. Furthermore, the transfer function in the output layer is governed by a linear function. Besides, the algorithm iteratively adjusts the link weights of the network and utilizes the Adam optimizer [26] in an effort to minimize the loss function of the neural network.

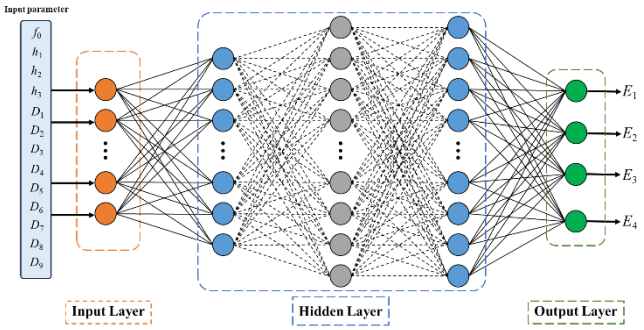

Fig. 2. Architectural framework of ANN.

2.2. Long Short-Term Memory (LSTM)

Hochreiter and Schmidhuber [27] introduced the Long Short-Term Memory (LSTM) neural network as an expansion of the recursive neural network architecture. Its primary purpose is to address gradient issues that may arise during reverse error training and to accommodate long-range data dependencies. A neuron and three gates—forget gates, input gates, and output gates—comprise the LSTM unit. The unit of the LSTM model is in neural network depicted in Fig. 3. The distinct input (x_t), long-term state (c_t), and short-term state (h_t) are presented in each time step t, respectively. The three gate formulations and the LSTM architecture are shown in the following equations:

$$f_t = \sigma\left(W_{xf} \cdot x_t + W_{hf} \cdot h_{t-1} + b_f\right) \quad (2)$$

$$i_t = \sigma\left(W_{xi} \cdot x_t + W_{hi} \cdot h_{t-1} + b_i\right) \quad (3)$$

$$o_t = \sigma\left(W_{xo} \cdot x_t + W_{ho} \cdot h_{t-1} + b_o\right) \quad (4)$$

$$g_t = \tanh\left(W_{xg} \cdot x_t + W_{hg} \cdot h_{t-1} + b_g\right) \quad (5)$$

$$c_t = f_t \cdot c_{t-1} + i_t \cdot g_t \quad (6)$$

$$y_t = h_t = o_t \cdot \tanh\left(c_t\right) \quad (7)$$

where $W_{xf}, W_{xi}, W_{xo}, W_{xg}$ are the connection weights with input $x_{(t)}$; $W_{hf}, W_{hi}, W_{ho}, W_{hg}$ are the connection weights with the previous short-term state $h_{(t-1)}$; b_f, b_i, b_o, b_g are the bias terms; and σ is sigmoid function.

The forget gate f_t, input gate i_t, and output gate o_t, based on the present input x_t and the previous short-term state h_{t-1} are evaluated using Eqs. (2) – (4), respectively. Additionally, the new candidate value g_t is appended to the cell state of the current time as presented in Eq. (5), and the past cell state c_{t-1} and previous short-term state h_{t-1} are updated by using Eqs. (6) – (7), respectively. The network generates predictions based on short-term state h_t, undergoes backpropagation to determine the discrepancy between the actual y_t and the predicted $\hat{y}_t$ values, computes gradients, and iteratively updates parameters utilizing Adam optimization algorithms [26] until convergence is attained.

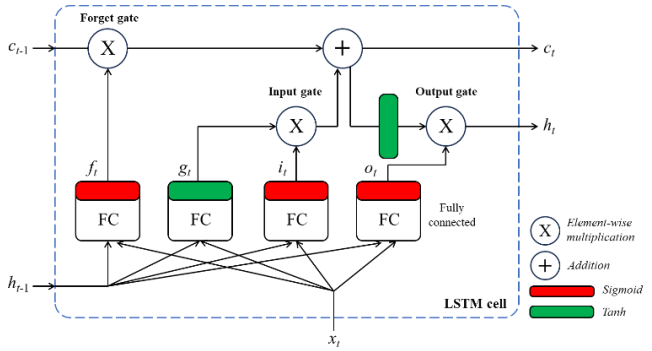

Fig. 3. Basic unit of LSTM.

2.3. Random Forest (RF)

Random Forest (RF) is a technique that combines numerous decision trees in order to generate greater accuracy and reliable prediction. RF, which was developed by Breiman [28] and Cutler et al. [29], is particularly advantageous when attempting to analyze complicated datasets with an abundance of variables. This is a result of its capacity to precisely model non-linear relationships between input and output, resulting in more accurate predictions. By constructing a multiplicity of decision trees, the RF approach attempts to separate the set used for training to minimize the mean squared error (MSE), and the output is the mean predicted outcome of the individual trees. Figure 4 illustrates the architectural framework of the RF model, which comprises of three primary components and steps: the construction of multiple decision trees, the selection of features, and the aggregation of predictions.

Step 1: The RF model utilizes the bootstrapping method to generate numerous decision trees, randomly selecting different subsets of the training data and replacing them with new data for ensuring that each tree is trained on a diverse portion of the dataset.

Step 2: Diversity among trees is introduced by selecting a random subset of features to evaluate divides at each node during each decision tree construction. This prevents the model from being dominated by a single feature and improves its capacity to capture complicated data patterns.

Step 3: The average value of each individual tree's prediction is used to calculate the predicted result.

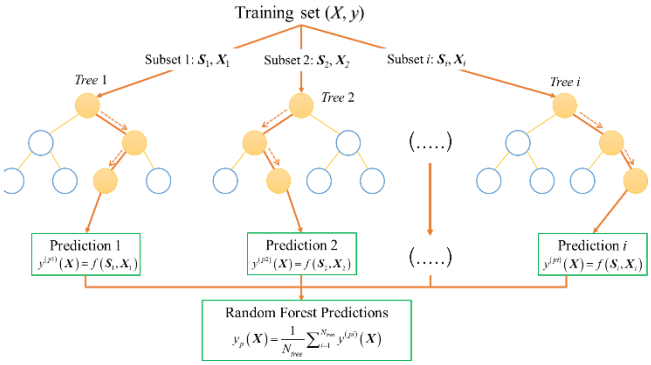

Fig. 4. Architectural framework of RF.

3. Methodology

The methodology employed in the development of machine learning models is outlined in this section. Figure 5 illustrates the process of constructing the ML model for backcalculating layered modulus of elasticity for the four-layered flexible pavement from FWD test data.

3.1. Synthetic Dataset

In the construction of a synthetic database for the machine learning model development, an analytical model of FWD test where a multi-layered elastic medium under a uniform load applied vertically over a circular area on its surface is considered as shown in Fig. 1. The multilayered elastic depicted in Fig. 1 is a system of four-layered flexible pavement found commonly in Thailand's road infrastructure. The pavement structure encompasses three finite layers of asphaltic concrete, base, and subbase, laying over an infinite subgrade medium. The deflections on the pavement surface in various radial directions under vertical loading are the necessary information for the construction of a synthetic database. The exact stiffness matrix (ESM) scheme is adopted in this study. The ESM scheme is based on the assembly of the layer stiffness matrices containing the analytical general solutions in the Hankel transform domain for each layer. The inversion of the global stiffness matrix of the multi-layered medium together with an appropriate numerical integration yields the surface deflections on the multi-layered pavements. More details on ESM technique are given elsewhere [19-23].

To generate the synthetic database, the appropriate ranges for input variables, which include the layer thicknesses (h_1, h_2, h_3), elastic moduli (E_1, E_2, E_3, E_4), and the magnitude of applied loading (f_0) are chosen according

to the data during prior FWD experiments conducted in Thailand to assess the pavement conditions. Maximum and minimum values observed from the preceding FWD experiments are included in the selected ranges. A total of 20,000 datapoints are generated using the randomly generated uniform distribution [30]. Each of these datapoints contains all four layers elastic modulus, the layered thicknesses, and the magnitude of applied loading. The statistics pertaining to the input parameters simulated using the uniform distribution are presented in Table 1. The ESM scheme is then applied, using the generated 20,000 datapoints as the input parameters, to determine surface deflections at nine radial distances on pavement surface (0, 200, 300, 450, 600, 900, 1200, 1500, and 1800 mm). Note that the loading radius of a = 150 mm is considered in the ESM scheme. The summary statistics for the obtained deflections are shown in Table 2.

To ensure the practical acceptance of the ESM scheme, a comparison is made between the surface deflections obtained from the ESM scheme and the past FWD field tests conducted on road pavement structures in Thailand. The required parameters from the FWD test data are shown in Table 3, which are used as input parameters in the ESM algorithm to calculate the surface deflections of the four-layered pavement in Fig. 1 under uniform loading of 150 mm radius. Figure 6 provides a comparison between the surface deflections computed using ESM and those obtained from the recorded FWD field tests at nine radial distances from the center of uniform loading (0, 200, 300, 450, 600, 900, 1200, 1500, and 1800 mm). The field-measured data displays a significant correlation with the ESM deflections as shown in Fig. 6. This close agreement demonstrates the reliability and accuracy of the ESM in modeling pavement behavior, further validating its applicability for the development of ML models to backcalculate the pavement moduli from FWD test.

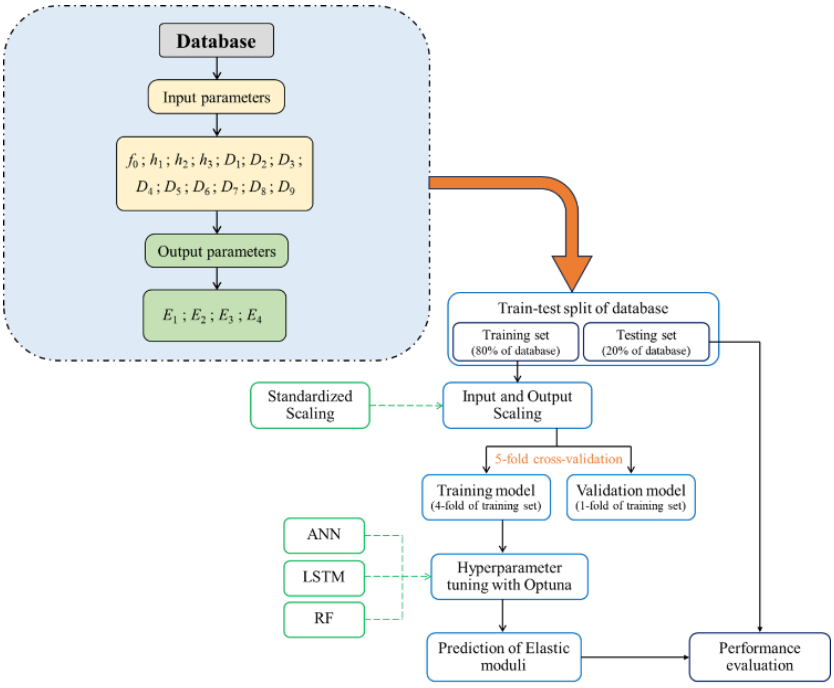

Fig. 5. Establishment of machine learning models.

Table 1. Descriptive statistics of input variables utilized in the construction of database.

Symbol	Description	Minimum	Maximum	Median	Average	Standard deviation
f_0 (kPa)	Uniformly distributed applied loading	700.004	799.998	750.587	750.294	28.854
E_1 (MPa)	Asphaltic concrete elastic modulus	1250.363	4999.826	3122.951	3125.29	1080.124
E_2 (MPa)	Base elastic modulus	175.007	699.978	435.072	435.737	151.494
E_3 (MPa)	Subbase elastic modulus	75.017	299.998	187.056	187.576	65.037
E_4 (MPa)	Subgrade elastic modulus	20.002	79.989	50.144	50.097	17.395
h_1 (mm)	Asphaltic concrete thickness	50.012	249.999	149.238	149.28	57.725
h_2 (mm)	Base thickness	100.009	299.994	200.103	200.081	57.882
h_3 (mm)	Subbase thickness	100.054	499.964	301.155	300.936	115.322

DOI:10.4186/ej.2025.29.3.27

Table 2. Descriptive statistics of generated deflections from ESM scheme at various locations.

Symbol	Description	Surface Deflections (μm)				
		Minimum	Maximum	Median	Average	Standard deviation
D_1	Center	333.122	3958.541	844.791	974.276	473.685
D_2	Center offset 200 mm	294.183	3134.122	726.249	817.859	377.961
D_3	Center offset 300 mm	272.666	2594.811	649.737	722.752	317.475
D_4	Center offset 450 mm	244.909	1949.861	539.715	607.43	251.906
D_5	Center offset 600 mm	221.774	1489.322	457.754	517.43	208.02
D_6	Center offset 900 mm	184.076	980.429	341.312	389.633	155.481
D_7	Center offset 1200 mm	149.914	741.26	266.86	305.9	124.862
D_8	Center offset 1500 mm	119.045	593.306	214.664	248.293	103.888
D_9	Center offset 1800 mm	99.04	494.713	178.087	207.004	88.204

Table 3. Input parameters for the exact stiffness matrix method (ESM) for the comparisons shown in Fig. 6.

Field Results	Asphaltic concrete			Base		Subbase		Subgrade
	f_0 (kPa)	h_1 (mm)	E_1 (MPa)	h_2 (mm)	E_2 (MPa)	h_3 (mm)	E_3 (MPa)	E_4 (MPa)
Section A	701	140	3714.3	150	355.73	250	161.99	42.06
Section B	711	50	3804.83	200	537.82	350	96.76	75.72
Section C	768	100	1660.19	230	498.51	200	295.91	29.53
Section D	786	90	2781.16	150	683.48	450	148.42	24.70

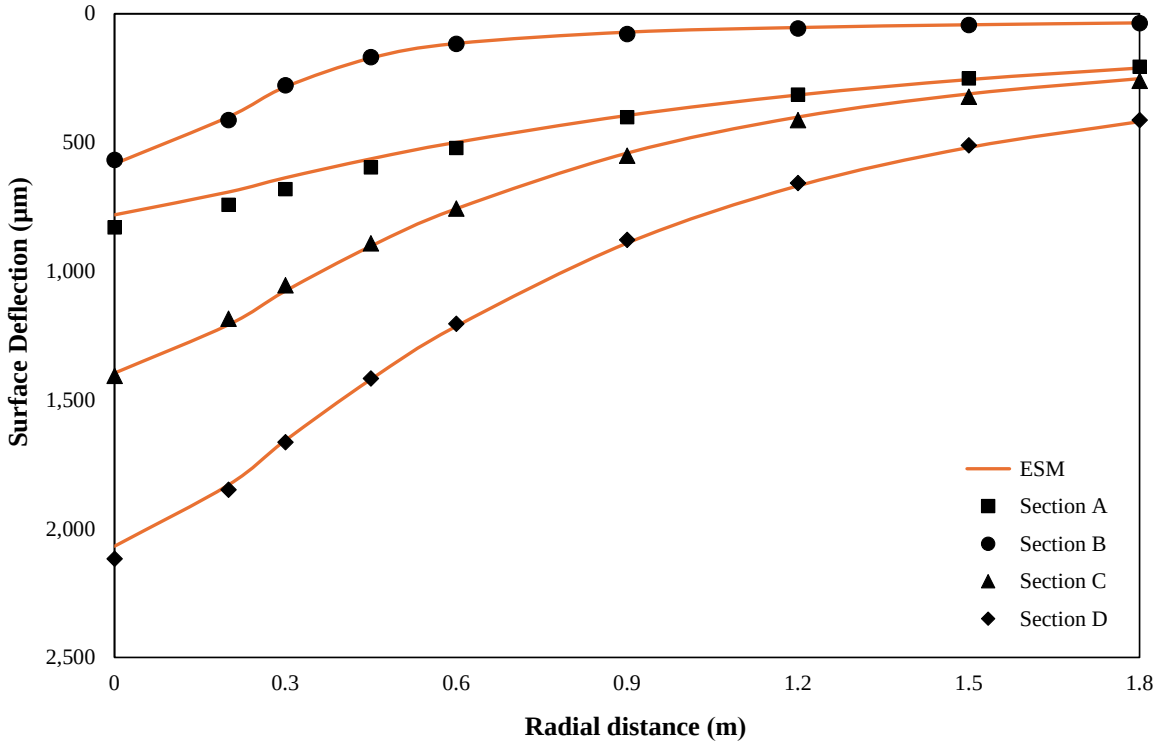

Fig. 6. Comparison between surface deflections at nine locations measured from the FWD test results and those computed from the exact stiffness matrix method (ESM).

3.2. Train-Test Split

The train-test split is an essential procedure in machine learning for assessing the effectiveness of a model. The generated database is branched into two portions, one designated for model training and the other specifically arranged for model's performance evaluation. The train set comprises 80% of the database (16,000 datapoints) and is employed for learning the model patterns and relationships within the data. In contrast, the test set, comprising 20% of the database (4,000 datapoints), is designated for the purpose of evaluating the model's capability to generalize the unobserved data. This approach guarantees that the model has undergone sufficient training with a substantial dataset, thereby facilitating its effective application to new FWD test data.

3.3. Data Scaling

Data scaling is a fundamental procedure in machine learning that simplifies the process of reducing the impact of anomalies and guaranteeing that all input and output variables are on a uniform scale. This stage is of crucial significance in order to reduce dimensional effects, enhance the models' precision, and accelerate convergence. To achieve this, the input and output variables are standardized to yield a zero mean and unit root mean square deviation, indicating that the data is centered on zero and has a variance of one. The procedure of standardization or Z-Score normalization is executed utilizing the following formula:

$$X' = \frac{X - \bar{X}}{S} \tag{8}$$

where X' denotes the standardized value resulting from scaling, X represents the original value, $\bar{X}$ is the average of the dataset, and S is the root mean square deviation of the dataset.

3.4. Hyperparameter Tuning and Cross-Validation

A crucial stage in the construction of machine learning models involves hyperparameter tuning along with cross-validation, which has significant impacts on the model performance. Hyperparameter optimization refers to the procedure of improving the ML model parameters that are selected prior to the initiation of the training process.

Optuna, a framework for Bayesian optimization, demonstrates itself as a dependable mechanism for automating hyperparameter improvements and enhancing model performance. By minimizing the average root mean square error (RMSE) in the set of validation the ML model, the Optuna approach facilitates the determination of the most effective hyperparameters [19, 31]. The Optuna technique is used to discover the most effective combination of hyperparameter values for machine learning models, allowing for various parameter selections within an appropriate space. This space is explored using five-fold cross-validation, which is employed to examine the ML model's robustness and generalizability. This is done by partitioning the training set, containing 80% of the database (16,000 datapoints), into five subsets. Four of these subsets (12,800 datapoints) are designated as the training model set, while the remaining subset (3,200 datapoints) is used to validate the model. By utilizing an iterative process, the model is able to effectively evaluate unseen data and prevent overfitting. Through combining hyperparameter optimization process with cross-validation, the predictive accuracy and reliability of the model are significantly enhanced during the development procedure. Table 4 represents the hyperparameters' optimal values for the construction of ANN, LSTM and RF models.

3.5. Model Performance Evaluation

The present investigation assesses machine learning models by employing various performance indicators, which includes root mean square error (RMSE), mean absolute percentage error (MAPE), and coefficient of determination (R^2), ratio of root mean square error to observations' standard deviation (RSR), index of scatter (IOS), and a20_index.

The squared average deviation among the predicted and actual values is denoted by RMSE; a lower RMSE indicates a more accurate prediction. MAPE measures the mean percentage discrepancy across the actual and predicted values, and a lesser MAPE indicates a more precise prediction. The value of R^2 indicates the level of precision with which the independent variables reflect the variability observed in the dependent variable. An R^2 value closer to 1 indicates the better performance of the model. The RSR varies between a large positive number and zero, which is the ideal value, representing the proportion between the RMSE and standard deviation of actual values. The effectiveness of the model is indicated by a lower value of RSR. In general, the IOS ranges from zero to infinity and represents the proportion between the RMSE and the mean of actual values. A lower IOS corresponds to a more accurate prediction. The a20_index, an indicator that varies from 0 to 100%, denotes the percentage of samples in which the variation among the predicted and actual values is greater than or equal to 20%. The above performance indicators are defined as follows:

$$\text{RMSE} = \sqrt{\frac{1}{n}\sum_{i=1}^{n}\left(y_i - \hat{y}_i\right)^2} \tag{9}$$

$$\text{MAPE} = \frac{1}{n}\sum_{i=1}^{n}\left|\frac{y_i - \hat{y}_i}{y_i}\right| * 100 \tag{10}$$

$$R^2 = 1 - \frac{\sum_{i=1}^{n}\left(y_i - \hat{y}_i\right)^2}{\sum_{i=1}^{n}\left(y_i - \frac{1}{n}\sum_{i=1}^{n} y_i\right)^2} \tag{11}$$

$$\text{RSR} = \frac{\text{RMSE}}{\sqrt{\frac{1}{n}\sum_{i=1}^{n}\left(y_i - \frac{1}{n}\sum_{i=1}^{n} y_i\right)^2}} \tag{12}$$

$$\mathrm{IOS} = \frac{\mathrm{RMSE}}{\frac{1}{n}\sum_{i=1}^{n} y_i} \quad (13)$$

$$\mathrm{a20\_index} = \frac{\mathrm{M20}}{n} * 100 \quad (14)$$

where n represents the amount of data; the actual and predicted values for the i^{th} datapoint are denoted by y_i and $\hat{y}_i$ respectively; M20 represents the quantity of samples in which the proportion of predicted to actual values lies within the interval of 0.8 to 1.2.

4. Data-Driven Solutions

The Python programming language [32] is utilized to construct the models of machine learning for data-driven solutions of the modulus of elasticity for the four-layered pavement structures based on the FWD experiment. Inside the models, the matrix of dependent variable **y** comprises the four elastic moduli, i.e., **y** = [E_1- E_4], whereas for the independent variables **X**, it contains the 13 input variables, i.e., **X** = [f_0; h_1-h_3; D_1-D_9].

4.1. Model Performance

Table 4 shows the optimal values of hyperparameters for the development of ML models. The ANN model contains five hidden layers, each containing an ideal number of neurons: 39, 45, 46, 35, and 50, with the learning rate of the model being 0.0022908. Furthermore, by setting the *L2* penalty parameter to 0.0004392, a regularization is proposed to penalize significant weights in order to avoid overfitting problem. Nonlinear learning is produced by the tanh activation function. The batch size contains 150 samples before updating the model's parameters. The training procedure encompasses a duration of 200 epochs, each of which represents an extensive iteration over the training dataset. Conversely, the LSTM model consists of four LSTM layers, each of which contains the following distribution of neurons: 80, 50, 59, and 42. The LSTM exhibits a slightly higher learning rate of 0.0027039 and a significantly lower *L2* penalty parameter of 0.0003511, which could reflect a balance between the model's complexity and the need to generalize well to new data. The activation functions employed through this network are tanh and sigmoid. Sigmoid may be utilized in the recurrent steps, while tanh is implemented within the LSTM gates in order to facilitate regulation of information flow within the network. The batch size in LSTM is 100, and similar to the ANN, the LSTM is also trained for 200 epochs.

Table 4. Hyperparameter optimization for the development of three ML models.

Model	Hyperparameter	Optimal Value
ANN	Hidden layer	5
	Node in each hidden layer	39-45-46-35-50
	Learning rate	0.0022908
	L2 penalty parameter	0.0004392
	Hidden layer activation function	tanh
	Output layer activation function	linear
	Batch Size	150
	Epochs	200
LSTM	Hidden layer of LSTM	4
	Node in each LSTM layer	80-50-59-42
	Learning rate	0.0027039
	L2 penalty parameter	0.0003511
	Hidden layer activation and recurrent functions	tanh, sigmoid
	Output layer activation function	linear
	Batch Size	100
	Epochs	200
RF	Number of trees	348
	Maximum depth	11
	Maximum features for the split	12
	Minimum samples split of internal node	6
	Minimum leaf node samples	4

The hyperparameter optimal value for the RF model is determined to reduce the discrepancy between the actual and predicted layered elastic modulus of the pavement, as demonstrated in Table 4. The hyperparameter's optimal value is obtained as follows: the number of estimators (348); the maximum depth (11); the maximum features for the split (12); the minimal internal node sample split allowed to divide (6); and the quantity of samples necessary for a leaf node (4). In order to propose a preliminary comparison of the performance from each ML model, a graphical illustration of the indicator of performance (R^2) for the estimation of layered elastic modulus by employing ANN, LSTM, and RF is illustrated in Figs. 7(a) and 7(b), according to the train set and test set, respectively. The evidence is apparent in Fig. 7 that the ANN and LSTM models clearly outperform the RF model for the prediction of the pavement layer elastic modulus. The R^2 values for the asphaltic concrete (E_1), base (E_2), and subbase (E_3) from the RF model are all lower than 60%, with only the R^2 value for the subgrade (E_4) being 98%. This indicates that the RF model is capable of successfully representing only the modulus of subgrade layer. In Phulsawat et al. [19], the RF model outperforms ANN in the prediction of all layer moduli. Note that only the measured surface deflections (D_1-D_9) are considered as the input variables in their study [19]. Thus, the increasing complexity of the relationships between the input variables (f_0; h_1-h_3; D_1-D_9) and the output variables (E_1-E_4) could be the reason why the RF model is unable to accurately predict the elastic moduli of all layers as more variables are introduced in the current analysis. Thus, only the results obtained from the ANN and LSTM models are considered in the subsequent analysis, interpretation, and discussion.

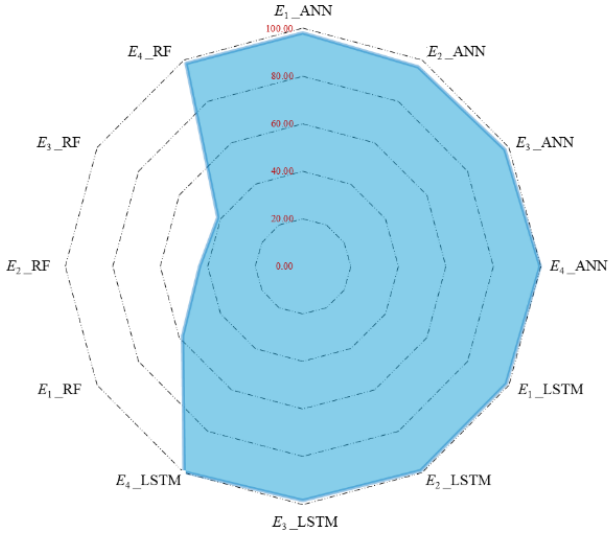

(a)

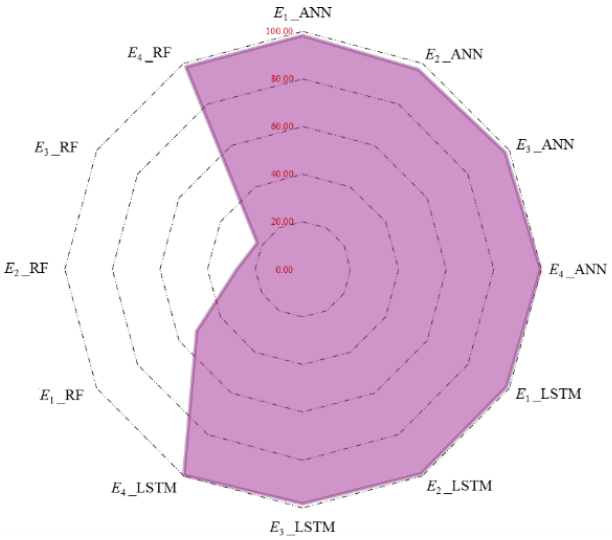

(b)

Fig. 7. Performance indicator (R^2) for ANN, LSTM, and RF models based on (a) train set; and (b) test set.

DOI:10.4186/ej.2025.29.3.27

Figure 8 shows scatter plots that represent the correlation between the input moduli of the ESM scheme to generate the synthetic database and the ANN model's prediction values both during the training and testing phases. With regard to the assessment of the model's performance, statistical tests, R^2, and MAPE values are shown. R^2 exceeds 96.5% for both datasets in the four-layered structure, and MAPE is lower than 4.8%, indicating an excellent level of accuracy. A considerable number of datapoints in each plot appear to be concentrated along the line of perfect agreement, indicating that the ANN model has achieved a precise assessment of all layered elastic modulus based on the FWD test. The close correspondence between the predicted moduli of elasticity obtained from ANN and the input moduli of elasticity in the exact stiffness matrix program indicates the predictive model has undergone adequate training, and it operates effectively.

The LSTM model's predicted modulus of elasticity for all layer pavement, utilizing optimal hyperparameters, is illustrated by the scatter plots for both the training and testing datasets as shown in Fig. 9. From a preliminary visual inspection, the LSTM model exhibits a scatter of points nearer to the diagonal line compared to what observed from the ANN model in Fig. 8. This implies that the LSTM model has a better capacity for accurate prediction than the ANN model. For the purpose of measuring the performance of the model, statistical tests, LSTM models exhibit extraordinary predictive ability (R^2 > 98.5% and MAPE < 3.2%) during both the training and testing stages, underscoring their exceptional accuracy in prediction the elastic moduli of all layers.

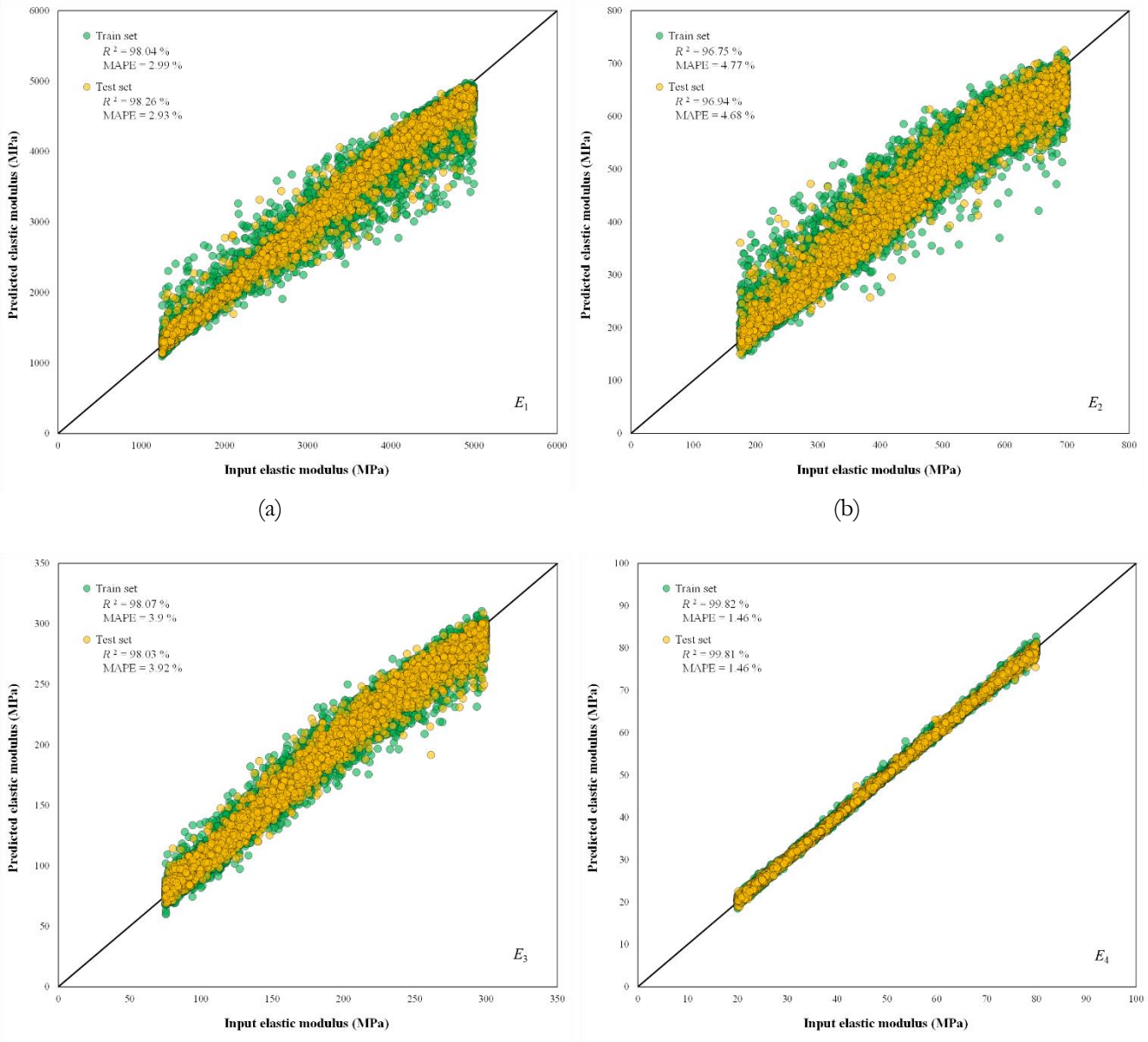

Fig. 8. Correlation between ANN predictions and input elastic moduli: (a) asphaltic concrete; (b) base; (c) subbase; and (d) subgrade.

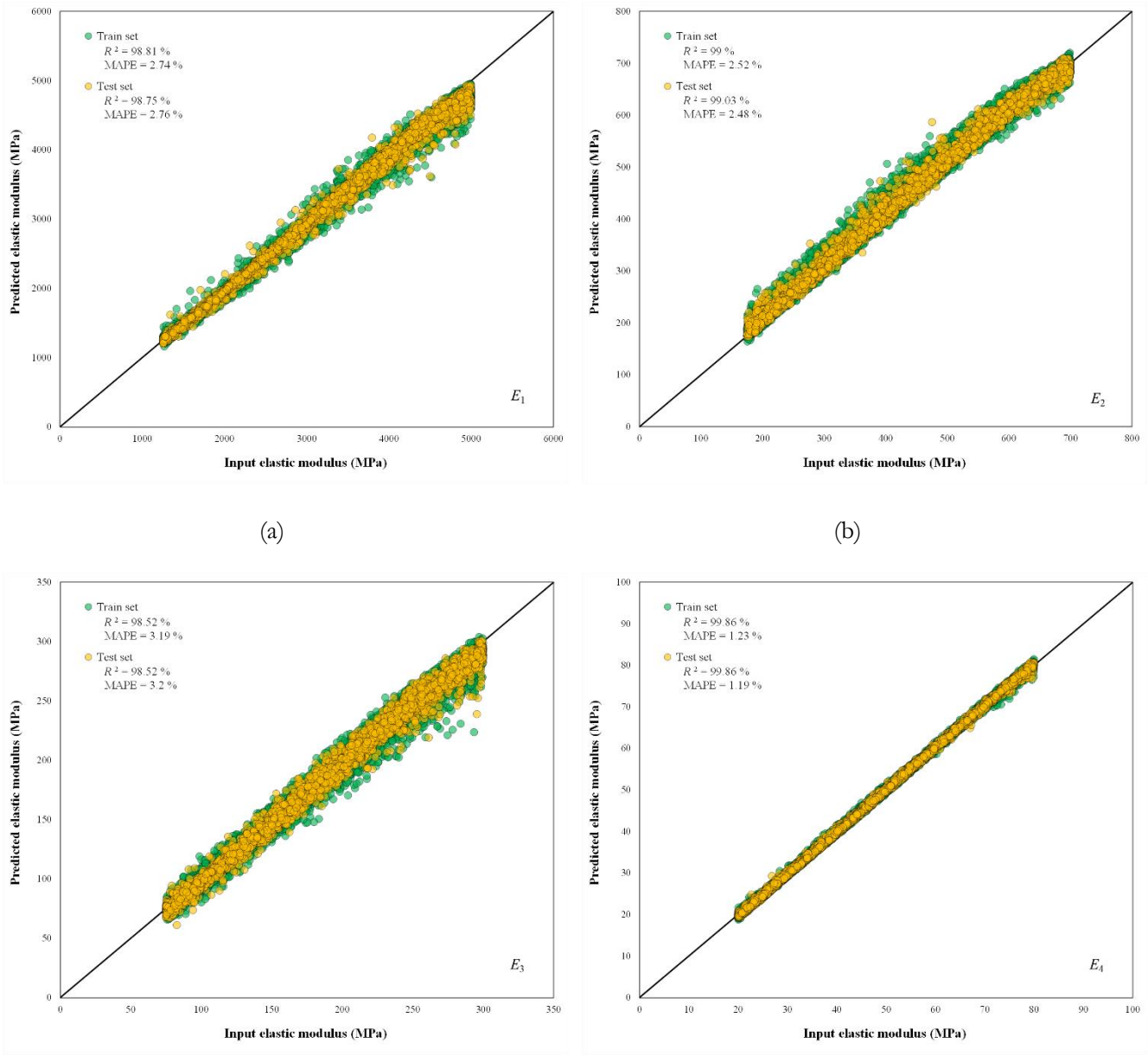

Fig. 9. Correlation between LSTM predictions and input elastic moduli: (a) asphaltic concrete; (b) base; (c) subbase; and (d) subgrade.

The efficiency of two machine learning models, ANN and LSTM, on their corresponding train and test sets is compared in Table 5. Throughout the training and testing stages, both models demonstrate exceptional predictive capabilities for the elastic moduli. Each dependent variable (E_1, E_2, E_3, and E_4) is comprehensively explained by all independent variables (f_0, h_1, h_2, h_3, and D_1-D_9), implying that there is a robust relationship between the input and output variables, ensuring that both models accurately capture underlying patterns. However, the LSTM model exhibits a slight edge over the ANN model across various indicators throughout the phases of training and testing due to its ability to capture long-term dependency patterns. When compared to the average values obtained from the ANN model (RMSE = 47.09 MPa, MAPE = 3.28%, R^2 = 98.17%, a20_index = 99.01%, RSR = 0.126, and IOS = 0.044), the average values from the LSTM model demonstrate lower RMSE (35.38 MPa), MAPE (2.42%), RSR (0.092), IOS (0.032), and a greater R^2 (99.05%), a20_index (99.96%) during the train stage. The LSTM model continues to outperform the ANN model during the test stage, as indicated through its lower RMSE (35.88 MPa), MAPE (2.41%), RSR (0.092), IOS (0.032), and a higher R^2 (99.04%), a20_index (99.94%) values, comparing to the corresponding average values obtained from the ANN model (RMSE = 44.57 MPa, MAPE = 3.25, and R^2 = 98.26%, a20_index = 99.09%, RSR = 0.122, and IOS = 0.042). Thus, the LSTM model exhibits superior performance in the prediction of the elastic moduli of flexible pavements based on FWD data. In the subsequent sections, the LSTM model is then employed in the verification with the data from FWD tests

carried out on Thailand's road infrastructure, and in the analysis of sensitivity to study the significant of each input variable on each layer's elastic modulus prediction.

4.2. Comparison with existing results

The applicability of the LSTM model is demonstrated by comparing the predicted elastic moduli with the backcalculated moduli from FWD field experiments carried out on Thailand's road infrastructure. In this investigation, 454 FWD test datapoints were selected from the previous FWD test on four-layered pavement sections with various thicknesses and different FWD loadings. In each datapoint, the applied loadings, layer thicknesses, and measured deflections from the nine geophones at a variety of locations were obtained from the test. It is essential to transmit these parameters to the LSTM model as the input variables in order to predict the elastic moduli of the four-layered pavement. Statistics values for the pavement sections derived from the FWD field testing are summarized in Table 6. Figure 10 illustrates a correlation between the elastic moduli predicted from the LSTM model and the backcalculated values obtained from the FWD field test results. The elastic moduli from the FWD tests were backcalculated from the ELMOD program using the measured surface deflections, the magnitude of applied loading, and the layer thicknesses obtained from the field tests. The ELMOD program was developed by Dynatest Consulting Inc., using the theory of Odemark-Boussinesqe transformed sections. It utilizes an iterative approach to estimate the elastic moduli by minimizing the discrepancy between measured and theoretical deflections derived at the pavement surface [33].

The accuracy and reliability of the LSTM model are explained by each subfigure, which concentrates on each layer material. A black diagonal line illustrates the ideal correlation, while dashed lines indicate acceptable deviations of +30%, +20%, -20%, and -30% between the predicted elastic moduli from the LSTM model and the backcalculated results from FWD field test. As shown in Fig. 10, it is evident that the majority of the datapoints for elastic moduli across all layers are distributed within a margin of error of ±20%, with a few exceeding the ±30% error lines. In the context of the overall performance measurement, the mean absolute percentage error (MAPE) indicates that the MAPE for the predicted elastic moduli of all pavement layers (E_1-E_4) do not exceed 15%, with the predicted subgrade modulus (E_4) exhibiting the lowest MAPE value of 9.88%. Thus, the LSTM model can be utilized as an acceptable alternative for predicting the multi-layered elastic moduli of pavement infrastructures according to FWD test data.

Table 5. Performance measures of the prediction of layered pavement moduli.

Dataset	Layer	Model	RMSE (MPa)	MAPE (%)	R^2 (%)	a20_index (%)	RSR	IOS
Train set	asphaltic	ANN	151.295	2.99	98.04	98.68	0.14	0.048
	concrete (E_1)	LSTM	117.863	2.74	98.81	99.99	0.109	0.038
	base (E_2)	ANN	27.271	4.77	96.75	97.68	0.18	0.063
		LSTM	15.108	2.52	99	99.93	0.1	0.035
	subbase (E_3)	ANN	9.041	3.9	98.07	99.68	0.139	0.048
		LSTM	7.909	3.19	98.52	99.91	0.122	0.042
	subgrade (E_4)	ANN	0.744	1.46	99.82	100	0.043	0.015
		LSTM	0.656	1.23	99.86	100	0.038	0.013
	Average	ANN	47.090	3.28	98.17	99.01	0.126	0.044
		LSTM	35.380	2.42	99.05	99.96	0.092	0.032
Test set	asphaltic	ANN	141.784	2.93	98.26	98.85	0.132	0.045
	concrete (E_1)	LSTM	119.962	2.76	98.75	99.98	0.112	0.038
	base (E_2)	ANN	26.615	4.68	96.94	97.85	0.175	0.061
		LSTM	14.99	2.48	99.03	99.93	0.098	0.035
	subbase (E_3)	ANN	9.121	3.92	98.03	99.68	0.14	0.048
		LSTM	7.903	3.2	98.52	99.85	0.122	0.042
	subgrade (E_4)	ANN	0.756	1.46	99.81	100	0.043	0.015
		LSTM	0.646	1.19	99.86	100	0.037	0.013
	Average	ANN	44.570	3.25	98.26	99.09	0.122	0.042
		LSTM	35.880	2.41	99.04	99.94	0.092	0.032

Table 6. Descriptive statistics of input variables from FWD experiments.

Symbol	Explanation	Minimum	Maximum	Median	Average	Standard deviation
f_0	Uniformly distributed applied loading	701	799	753	750.725	27.761
h_1	Asphaltic concrete's thickness	70	200	120	119.295	37.931
h_2	Base's thickness	150	250	200	206.718	37.47
h_3	Subbase's thickness	150	450	300	305.176	100.938
D_1	Uniform loading center	391.5	2897.4	965.1	1083.552	465.163
D_2	Center offset 200 mm	346.8	2403.2	805.05	913.03	397.428
D_3	Center offset 300mm	320.8	2085.8	698.75	804.916	353.051
D_4	Center offset 450 mm	285.3	1702.6	577.05	670.604	298.746
D_5	Center offset 600 mm	249.6	1408	477.85	564.047	255.658
D_6	Center offset 900 mm	191.8	980.1	344.85	411.898	192.391
D_7	Center offset 1200 mm	150.3	740.6	262.5	314.159	149.725
D_8	Center offset 1500 mm	119.2	590.6	209.3	249.381	119.869
D_9	Center offset 1800 mm	99.07	490.8	172.15	204.942	98.597

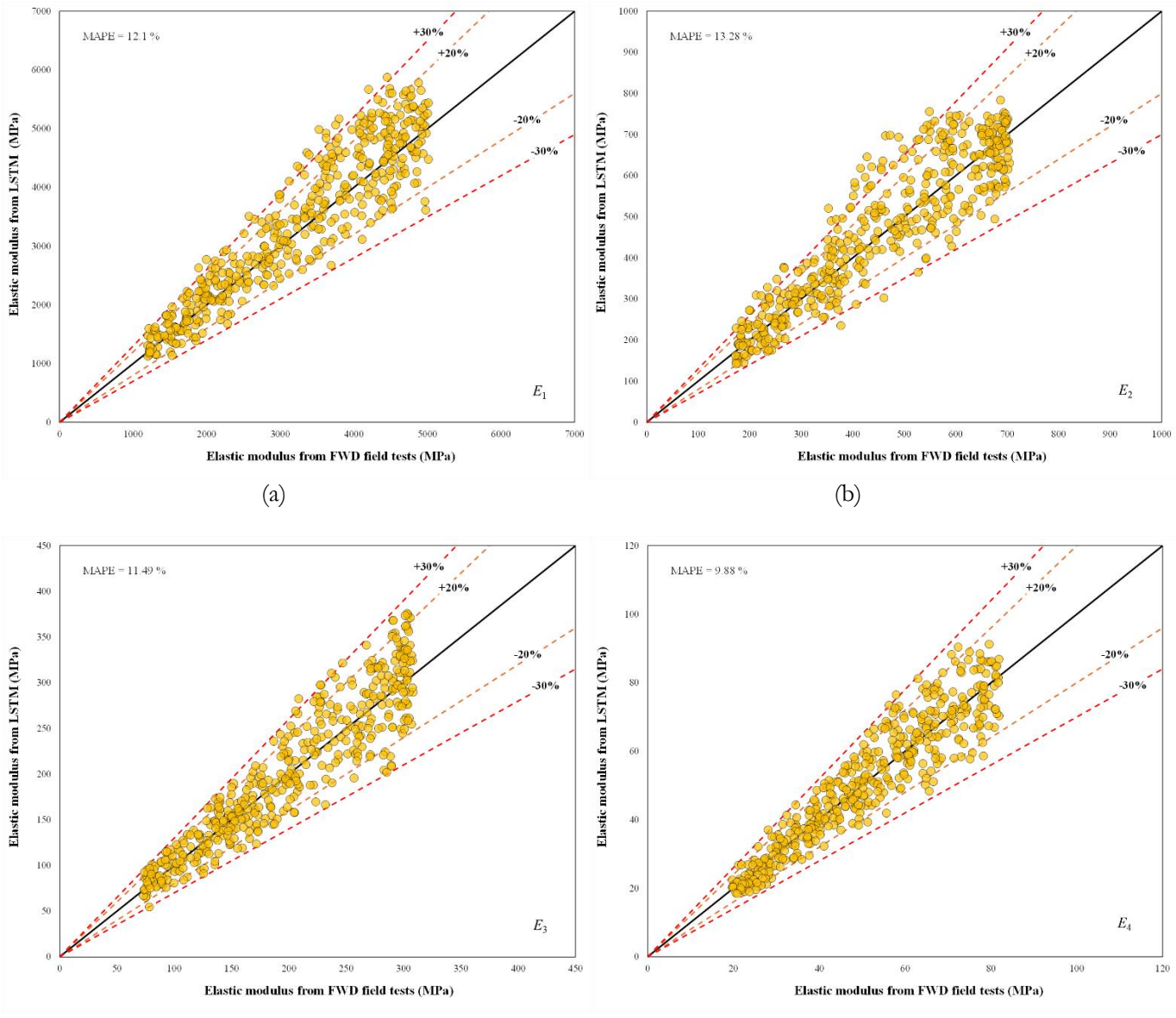

Fig. 10. Correlation between predicted elastic moduli from LSTM and backcalculated values from FWD field test: (a) asphaltic concrete; (b) base; (c) subbase; and (d) subgrade.

To further verify the present ML results, Table 7 presents a comparison between the predicted elastic moduli from LSTM and the conventional backcalculated scheme based on a nonlinear least square optimization based on modified Levenberg-Marquardt algorithm. Puarungroj [34] employed this scheme in the backcalculation for pavement layer moduli from FWD data using dynamic analysis. The backcalculated moduli from the past FWD field tests based on ELMOD are also presented for comparison. It is evident from Table 7 that, although there are several inconsistencies among the three schemes, the elastic moduli values generated by the LSTM model exhibit strong consistency with ELMOD, particularly for the asphaltic concrete (E_1) and base layer (E_2). This underscores the potential of the LSTM model as a viable alternative to conventional backcalculation techniques, given its ability to approximate backcalculated moduli from FWD tests with reasonable accuracy. Thus, LSTM can serve as a practical and efficient tool for backcalculating the elastic moduli of pavement structures, reducing the computational complexity associated with conventional backcalculation methods while maintaining accuracy and reliability.

4.3. Sensitivity Analysis

This subsection presents sensitivity analysis to assess the relative significance of each input variable, i.e. the magnitude of uniform vertical loading (f_0), the layer thicknesses (h_1, h_2, h_3), and measured surface deflections (D_1-D_9), on the estimation of layered elastic moduli (E_1-E_4). Plischke [35] performed the first-order sensitivity analysis, employing the Fourier Amplitude Sensitivity Test (FAST) in conjunction with the Efficient Approximation of Sensitivity Indices (EASI) and Random Balance Designs (RBD). A bias correction technique which Tissot and Prieur [36] is additionally adopted to improve the accurateness of sensitivity estimates. The formula for determining the first-order sensitivity of an input variable is expressed as follows:

$$S_i = \frac{\mathrm{V}\left[E\left(f\left(\hat{y}, X_i\right)\right)\right]}{\mathrm{V}[\hat{y}]} \tag{15}$$

where V[.] represents the variation in values of a random variable and E (f (y, X_i)) denotes the conditioned expectation of the machine learning predicted value for a given X_i. A robust correlation between the predicted output variable $\hat{y}$ and the input parameter X_i is indicated by a high value of S_i.

In the current study, the sensitivity analysis is conducted by representing the first-order sensitivities of input parameters on the predicted elastic moduli from LSTM model, as presented in Fig. 11. It is evident from Fig. 11 that the first-order sensitivities of the loading magnitude (f_0) and the layer thicknesses (h_1-h_3) are relatively low across all predicted layered moduli, suggesting that the input variables f_0 and h_1-h_3 have less impact on E_1-E_4 compared to the measured surface deflections on (D_1-D_9). For the asphaltic concrete layer (E_1), the measured deflections at D_1 predominantly influence the prediction of E_1, with the highest first-order sensitivity at 48%, followed by D_2 and D_3, with sensitivities of 21.74% and 13.77%, respectively. In addition, the deflections at the remaining geophones (D_4 to D_9) contribute only marginally, with sensitivity values below 8%. Similarly, the deflections measured at the center of loading D_1 exhibit the most significant influence on the base layer modulus (E_2), followed by the deflections at D_2 and D_3, respectively. It is found that the cumulative effect of the deflections observed at the first three geophones (D_1 to D_3) on the estimated value of E_2 exceeds 70%.

Table 7. Comparison of backcalculated elastic moduli from various schemes.

Section	f_0 (kPa)	Layer	Thickness (mm)	Backcalculation Moduli (MPa)		
				ELMOD	Levenberg-Marquardt	LSTM
A	704	asphaltic concrete (E_1)	200	2980.674	2978.265	3035.977
		base (E_2)	250	377.346	387.184	372.049
		subbase (E_3)	300	184.484	96.793	185.519
		subgrade (E_4)	∞	50.536	50.397	50.233
B	757	asphaltic concrete (E_1)	100	4879.248	4949.369	4974.01
		base (E_2)	200	229.658	223.63	224.538
		subbase (E_3)	350	227.704	132.078	238.363
		subgrade (E_4)	∞	31.26	38.578	31.234
C	763	asphaltic concrete (E_1)	120	2872.408	2141.029	2842.911
		base (E_2)	150	272.145	482.595	279.291
		subbase (E_3)	450	293.531	182.215	298.567
		subgrade (E_4)	∞	63.686	63.709	63.253
D	797	asphaltic concrete (E_1)	200	1434.954	1397.39	1564.69
		base (E_2)	250	251.024	280.296	249.843
		subbase (E_3)	350	121.196	70.805	127.394
		subgrade (E_4)	∞	21.999	21.859	22.861

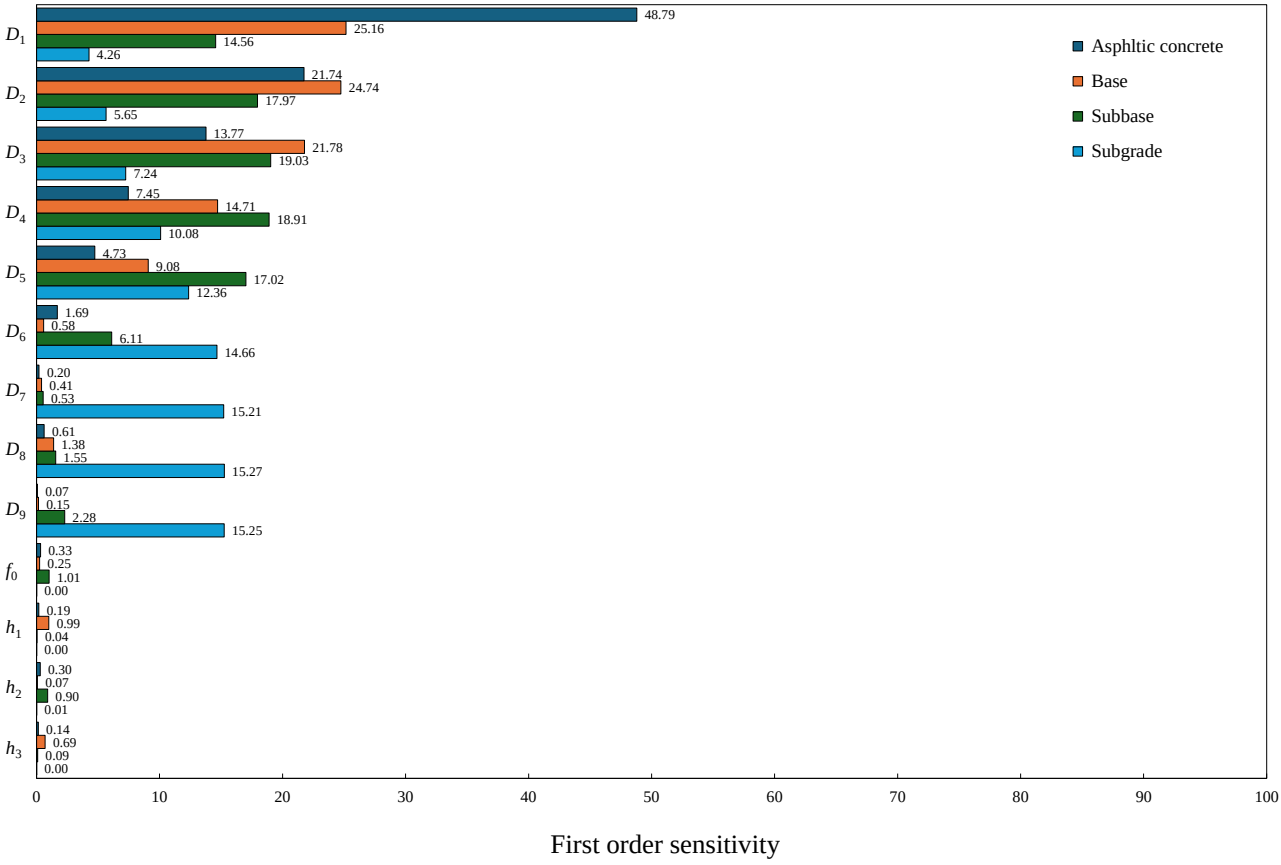

Fig. 11. First-order sensitivity of measured deflections on the predicted moduli from LSTM.

Figure 11 also reveals that the subbase modulus (E_3) is dominated by the deflections at D_1 to D_5, with sensitivities ranging from 14% to 19%, while sensitivities from D_6 to D_9 lie between 2% to 6%. This pattern suggests that, unlike E_1 and E_2, the influential deflections on E_3 extend beyond the first three geophones. For the subgrade modulus, no single geophone dominates the prediction of E_4, with the sensitivities of D_4 to D_9 being from 10% to 15%. The results from the sensitivity analysis are consistent with Zhang et al. [37], who performed a dynamic analysis to determine displacement fields from a theoretical model of a three-layered pavement structure under FWD loading and provided a precondition for the backcalculation of multilayered pavement moduli. They found the variation of elastic modulus of the top surface mainly influences the vertical displacement of points close to the load center. The vertical displacement affected by the elastic modulus of the base course is shown in a broader range, while the subgrade effect is observed across the entire monitoring area.

5. Conclusions

This research focuses on the development of data-driven solutions for backcalculating the modulus of elasticity for multi-layered pavement structures from the Falling Weight Deflectometer (FWD) experiment. Various machine learning techniques, namely, artificial neural network (ANN), long short-term memory (LSTM), and random forest (RF), are effectively established from a synthetic database for the backcalculation process. The exact stiffness matrix scheme is employed to create an exhaustive database containing 20,000 flexible pavements of four-layered roadway structures. The developed machine learning models utilize the following input variables: the applied uniform vertical loading (f_0); the thicknesses of the top three layers (h_1, h_2, h_3); and the surface deflections, which are measured at nine different locations (D_1 to D_9). The estimation of four-layered elastic modulus (E_1 to E_4) constitutes the output variables. All hyperparameters are meticulously optimized in an effort to minimize the loss function between the predicted and input elastic moduli in the construction of the ML models.

Among the three proposed ML algorithms, the ANN and LSTM models outperform the RF model in terms of capturing complex relations for the purpose of estimating the four-layered pavement elastic moduli, while maintaining an exceptionally high level of accuracy. Various statistical metrics, namely, RMSE, MAPE, R^2, RSR, IOS, a20_index, are implemented to evaluate the performance of the developed ANN and LSTM models, and they reveal that both constructed models exhibit outstanding performance. However, the LSTM model demonstrates superior performance compared to the ANN model. The increased reliability of the LSTM model signifies consistent performance across various datasets, whereas its enhanced accuracy assures more accurate predictions of the layered pavement moduli. Additionally,

the LSTM model demonstrates reduced variability, implying that its predictions are more stable and less impacted by variations in the input.

The aforementioned characteristics collectively support the LSTM model as a more robust and reliable instrument for backcalculating modulus of elasticity in the four-layered pavement structures based on FWD test on road infrastructures. Furthermore, the comparison between the predicted moduli from the LSTM model and the backcalculated moduli from the FWD experiment indicates an acceptable agreement, with the MAPE for all predicted modulus (E_1-E_4) is less than 15%. Thus, the developed LSTM model exhibits an impressive accuracy for backcalculating the four-layered pavement moduli based on the FWD test.

The sensitivity analysis reveals that the measured deflections at center of uniform vertical load (D_1) exhibit the most significant influence on the prediction of the elastic modulus of asphaltic concrete and base layer (E_1 and E_2), while the measured deflections at D_2 and D_3 also contribute substantially to the prediction of the base layer modulus (E_2). Conversely, the prediction of the subbase and subgrade moduli (E_3 and E_4) is not significantly influenced by any particular measured deflections. Besides, the layer thickness and the magnitude of vertical loading have negligible effects on the estimation of the pavement elastic moduli. The present findings emphasize the efficacy of the LSTM model and offer significant insights into the behavior of multi-layered flexible pavements, thereby enhancing the assessment of road infrastructures.

The efficiency of developed ML models presented in this paper illustrates the prospective applications of data-driven approaches to the strength assessment of transportation infrastructure networks for preventive maintenance. Work is currently underway to generate anomaly detection algorithms integrated with the developed ML model to filter out outliers in measured deflections obtained from FWD field tests. This will enhance the accuracy and reliability of the predicted multi-layered pavement moduli in the backcalculation process based on FWD test results.

Acknowledgement

This research was funded by The Royal Golden Jubilee Scholarship (grant number NRCT5-RGJ63001-010).

References

[1] A.M. Ebid, "35 Years of (AI) in geotechnical engineering: state of the art," *Geotechnical and Geological Engineering*, vol. 39, pp. 637–690, 2021.

[2] N.T. Ngo, H.A. Le, V.V. Huynh, and T.P.T. Pham, "Machine learning models for inferring the axial strength in short concrete-filled steel tube columns infilled with various strength concrete," *Engineering Journal*, vol. 25, no. 7, pp. 135–145, 2021.

[3] J. Khatti, H. Samadi, and K.S. Grover, "Estimation of settlement of pile group in clay using soft computing techniques," *Geotechnical and Geological Engineering*, vol. 42, pp. 1729–1760, 2024.

[4] K. Yoonirundorn, T. Senjuntichai, S. Keawsawasvong, C. Ngamkhanong, and A.C. Wijeyewickrema, "Stability analysis of multiple unsupported excavations in cohesive-frictional soils using finite element limit analysis (FELA) and an artificial neural network (ANN)," *Modeling Earth Systems and Environment*, vol 10, pp. 1589–1598, 2024.

[5] F. Kong, X. Zhou, C. Guo, D. Lu, and X. Du, "Elastic analytical method with machine learning for predicting the stratum displacement field induced by shallow tunneling," *Engineering Analysis with Boundary Elements*, vol. 159, pp. 201–212, 2024.

[6] A. Roshan and M. Abdelrahman, "Improving aggregate abrasion resistance prediction via micro-deval test using ensemble machine learning techniques," *Engineering Journal*, vol. 28, no. 3, pp. 15–24, 2024.

[7] S. Ramadan, H. Kassem, A. ElKordi, and R. Joumblat, "Incorporating artificial intelligence applications in flexible pavements: A comprehensive overview," *International Journal of Pavement Research and Technology*, 2024.

[8] W. Zeiada, L. Obaid, S. El-Badawy, R.A. El-Hakim, and A.M. Awed, "Benchmarking classical and deep machine learning models for predicting hot mix asphalt dynamic modulus," *Civil Engineering Journal*, vol. 11, no. 1, pp. 76–106, 2025.

[9] D. Eustace, B. Naik, H. Wei, and P. Bhavsar, *Emerging transportation safety and operations: Practical perspectives*. Switzerland: MDPI, 2025.

[10] R.W. Meier and G.J. Rix, "Backcalculation of flexible pavement moduli using artificial neural networks," Transportation Research Record, TRB, National Research Council, Washington, D.C., United States, 1994, pp. 75–82.

[11] R.W. Meier and G.J. Rix, "Backcalculation of flexible pavement moduli from dynamic deflection basins using artificial neural networks," Transportation Research Record, Transportation Research Record. TRB, National Research Council, Washington, D.C., United States, 1995, pp. 72–81.

[12] S. Sharma and A. Das, "Backcalculation of pavement layer moduli from falling weight deflectometer data using an artificial neural network," *Canadian Journal of Civil Engineering,* vol. 35, no. 1, pp. 57–66, 2008.

[13] J.M. Gonzalez, J.M. Carbonell, and W. Van Bijsterveld, "Evaluation of multilayer pavement viscoelastic properties from falling weight deflectometer using neural networks," in *Transport Research Arena (TRA) 5th Conference: Transport Solutions from Research to Deployment*, Paris, France, 2014

[14] F. Leiva-Villacorta, A. Vargas-Nordcbeck, and D.H. Timm, "Non-destructive evaluation of sustainable pavement technologies using artificial neural

networks," *International Journal of Pavement Research and Technology*, vol. 10, no. 2, pp. 139–147, 2017.

[15] A.R. Ghanizadeh and M. Padash, "Nonlinear backcalculations of inverted pavements using hybrid artificial neural network and colliding body optimization algorithm," *Journal of Transportation Infrastructure Engineering*, vol. 5, no. 4, pp. 111–132, 2019.

[16] A.R. Ghanizadeh, N. Heidarabadizadeh, and F. Jalali, "Artificial neural network back-calculation of flexible pavements with sensitivity analysis using Garson's and connection weights algorithms," *Innovative Infrastructure Solutions*, vol. 5, no. 63, 2020.

[17] A.R. Ghanizadeh, N. Heidarabadizadeh, and V. Khalifeh, "Developing a hybrid ANN-Jaya procedure for backcalculation of flexible pavements moduli," *Civil Engineering Infrastructures Journal*, vol. 55, no. 1, pp.89–108, 2022.

[18] C. Han, T. Ma, C. Siyu, and F. Jianwei. "Application of a hybrid neural network structure for FWD backcalculation based on LTPP database," *International Journal of Pavement Engineering*, vol. 23, no. 9, pp. 3099–3112, 2022.

[19] B. Phulsawat., A. Senjuntichai, and T. Senjuntichai, "Prediction of multi-layered pavement moduli based on falling weight deflectometer test using soft computing approaches," *Transportation Infrastructure Geotechnology*, 2024.

[20] T. Senjuntichai, N. Sornpakdee, J. Teerawong, and RNKD. Rajapakse. "Time dependent response of an axially loaded elastic bar in a multi-layered poroelastic medium," *Journal of Engineering Mechanics*, ASCE., vol. 133, no. 5, pp. 578–587, 2007.

[21] T. Senjuntichai, and W. Kaewjuea. "Dynamic response of multiple flexible strips on a multilayered poroelastic half-plane," *Journal of Mechanics and Materials of Structures*, vol. 3, no. 10, pp. 1885–1901, 2008.

[22] T. Senjuntichai, S. Keawsawasvong, and Bundid Yooyao, "Exact stiffness method for multi-layered saturated soils under moving dynamic loads," *Journal of GeoEngineering*, vol. 15, no. 3, pp. 159-171, 2020.

[23] T. Senjuntichai, B. Phulsawat, S. Keawsawasvong, and RNKD. Rajapakse, "Vertical vibration of an embedded flexible foundation in multi-layered transversely isotropic saturated," *Computers and Geotechniques*, vol. 172, p. 106399, 2024

[24] W.S. McCulloch and W. Pitts, "A logical calculus of the ideas immanent in nervous activity," *The Bulletin of Mathematical Biophysics*, vol. 5, pp. 115–133, 1943.

[25] N. Metropolis, A.W. Rosenbluth, M.N. Rosenbluth, A.H. Teller, and E. Teller, "Equation of state calculations by fast computing machines," *The Journal of Chemical Physics*, vol. 21, no. 6, pp. 1087–1092, 1953.

[26] D.P. Kingma and J. Ba, "Adam: A method for stochastic optimization," in *Proceedings of the 3rd International Conference for Learning Representations*, San Diego, 2015, pp. 1–15.

[27] S. Hochreiter and J. Schmidhuber, "Long short-term memory," *Neural Computation*, vol. 9, no. 8, pp. 1735–1780, 1997

[28] L. Breiman, "Random forests," *Machine Learning*, vol. 45, pp. 5–32, 2001.

[29] A. Cutler, D.R. Cutler, and J.R. Stevens, "Random forests," in *Ensemble Machine Learning: Methods and Applications*, C. Zhang and Y. Ma, Eds.New York: Springer, 2012, pp. 157–175.

[30] V.P. Singh, "Uniform distribution," in *Entropy-Based Parameter Estimation in Hydrology*. *Water Science and Technology Library*, *vol. 30*. Dordrecht: Springer, 1998.

[31] T. Liu, Z. Wang, J. Zeng, and J. Wang, "Machine-learning-based models to predict shear transfer strength of concrete joints," *Engineering Structures*, vol. 249, 2021.

[32] G.V. Rossum and F.L. Drake, *Python Tutorial*. The Netherlands: Centrum voor Wiskunde en Informatica Amsterdam, 1995.

[33] M. Ameri, N. Yavari, and T. Scullion, "Comparison of static and dynamic backcalculation of flexible pavement layers moduli using four softwares," *Asian Journal of Applied Sciences*, vol. 2, no. 3, pp. 197–210, 2009.

[34] W. Puarungroj, "Backcalculation for pavement layer moduli from FWD data using dynamic analysis," Master's degree thesis, Department of Civil Engineering, Faculty of Engineering, Chulalongkorn University, 2001.

[35] E. Plischke, "An effective algorithm for computing global sensitivity indices (EASI)," *Reliability Engineering* & *System Safety*, vol. 95, no. 4, pp. 354–360, 2010.

[36] J.Y. Tissot and C. Prieur, "Bias correction for the estimation of sensitivity indices based on random balance designs," *Reliability Engineering* & *System Safety*, vol. 107, pp. 205–213, 2012.

[37] J. Zhang, Z. Lu, C. Tang, J. Liu, and H. Yao, "Forward calculation of displacement fields with multilayered unsaturated highway system induced by falling weight deflectometer using dynamic response method," *Transportation Geotechnics*, vol. 38, p. 100866, 2023.

Barami Phulsawat was born in Nakhon Si Thammarat, Thailand in 1997. He received the Bachelor's degree in Civil Engineering from Prince of Songkla University, Hat Yai, Thailand in 2019. Currently, he is a Doctor of Philosophy degree in Civil Engineering, Chulalongkorn University, Bangkok, Thailand. His research interests involve in solid and structural mechanics, contact mechanics, civil engineering, and machine learning.

Teerapong Senjuntichai obtained his B. Eng. (Civil Engineering) from Chulalongkorn University in 1988; M. Eng. (Structural Engineering) from Asian Institute of Technology in 1990; and Ph.D. (Civil Engineering) from The University of Manitoba in 1994. He has then joined the Department of Civil Engineering, Chulalongkorn University, where he is currently a full-time professor. He was a post-doctoral associate at The University of Minnesota from 1997-1999. His fields of specialization are applied mechanics, geomechanics, and structural engineering. Prof. Senjuntichai has served as an editorial board member in several international journals and also a Head of Center of Excellence in Applied Mechanics and Structures, Chulalongkorn University.

Angsumalin Senjuntichai obtained her first degree in industrial engineering (B.Eng.) from Chulalongkorn University in 1994. She received a master degree in industrial engineering (M.S.I.E.) from The University of Minnesota in 1999, and a doctoral degree in industrial engineering (D.Eng) from Asian Institute of Technology in 2011. In 1994, she has joined the Department of Industrial Engineering, Chulalongkorn University where she is currently an associate professor and Head of Department. Dr. Senjuntichai has been constantly involved in professional activities. She has served as a technical consultant to several governments and private sectors for various engineering projects. Her interested fields are applied statistics, financial engineering, and data analytics.

Wichairat Kaewjuea was born in Krabi, Thailand in 1990. He received the Bachelor's degree in Civil Engineering from Prince of Songkla University in 2000. He received the Master's and Doctoral's degrees in Civil Engineering from Chulalongkorn University in 2004 and 2011, respectively. He is currently an Assistant Professor at Department of Civil Engineering, Prince of Songkla University, Hat Yai, Thailand. His research interests are in the areas of solid and structural mechanics, geomechanics, and structural engineering.